

Carbon isotope anomaly and other geochemical changes at the Triassic-Jurassic boundary from a marine section in Hungary

József Pálffy* Museum für Naturkunde, Universität zu Berlin, Invalidenstrasse 43, D-10115 Berlin, Germany

Attila Demény Laboratory for Geochemical Research, Hungarian Academy of Sciences, Budaörsi út 45, H-1112 Budapest, Hungary

János Haas Geological Research Group, Hungarian Academy of Sciences, Múzeum krt 4/a, H-1088 Budapest, Hungary

Magdolna Hetényi University of Szeged, Department of Mineralogy, Geochemistry and Petrology, POB 651, H-6701 Szeged, Hungary

Michael J. Orchard Geological Survey of Canada, 101-605 Robson Street, Vancouver, British Columbia V6B 5J3, Canada

István Vető Hungarian Geological Institute, Stefánia út 14, H-1143 Budapest, Hungary

ABSTRACT

Most mass extinctions are linked with carbon isotope excursions, implying that biotic crises are coupled with changes in the global carbon cycle. The isotopic evolution during the end-Triassic extinction is far less documented than that for the other major Phanerozoic extinctions. Here we report a sharp and short-lived -3.5% excursion in carbon isotope values for carbonate ($\delta^{13}\text{C}_{\text{carb}}$) corresponding to a -2% excursion in the isotopic composition of marine organic matter ($\delta^{13}\text{C}_{\text{org}}$) and other geochemical changes from the topmost Triassic in the Csóvár section in Hungary. The Triassic-Jurassic boundary is defined by ammonoid and conodont biostratigraphy in a marine limestone sequence. A decline in primary productivity, release of methane through dissociation of gas hydrates, or a combination of the two may account for the correlative biotic and isotopic events.

Keywords: Triassic, Jurassic, extinction, stable isotopes, carbon cycle.

INTRODUCTION

Pronounced isotopic excursions are associated with most of the major extinction events, giving support to causal linkage of biotic and environmental perturbations (Hallam and Wignall, 1997). The end-Triassic extinction is the least well understood event among the five largest Phanerozoic extinctions (Hallam, 1996). Its magnitude is exemplified by the loss of conodonts, near elimination of ammonoids, decimation of reef ecosystems, and severe turnover in terrestrial faunas and floras. However, the stable isotope record across the Triassic-Jurassic (Tr-J) boundary has remained poorly known until recently, denying an important test for various causal hypotheses.

Stable isotope studies have been reported from only three of the few known marine boundary sections. McRoberts et al. (1997) documented a small negative $\delta^{13}\text{C}_{\text{carb}}$ anomaly from the boundary interval in the Lorüns section in Austria. Also in Austria, at Kendlbachgraben, a negative $\delta^{13}\text{C}_{\text{carb}}$ excursion is confined to the lithologically distinctive boundary marl unit and is accompanied by a positive $\delta^{13}\text{C}_{\text{org}}$ and a negative $\delta^{18}\text{O}$ excursion, indicating diagenetic overprint (Hallam and Goodfellow, 1990; Morante and Hallam, 1996). A negative $\delta^{13}\text{C}_{\text{org}}$ anomaly, coinciding with the end-Triassic radiolarian extinc-

tion, was reported from the Queen Charlotte Islands (Ward et al., 2001). Organic carbon isotopic data from a terrestrial section in Greenland also hint at a negative carbon excursion at the boundary (McElwain et al., 1999).

Herein we report the results of an integrated biostratigraphic, sedimentologic, and geochemical study from a marine Tr-J boundary section at Csóvár, Hungary (Pálffy and Dosztály, 2000). Ammonoid and conodont biostratigraphy is presented to define the position of the system boundary. Microfacies analysis helps interpret the depositional environment and track facies changes throughout the boundary interval. Finally, the carbon and oxygen isotopic evolution is reconstructed from bulk carbonate and bulk organic matter samples, supplemented with organic geochemical analyses. These results yield a stable isotope curve for the Tr-J transition and shed new light on the coupled environmental and biotic changes at this extinction event.

GEOLOGIC SETTING

Northeast of Budapest, in north-central Hungary, the Mesozoic basement crops out only in a few small, fault-bounded blocks that belong to the Transdanubian Range tectonic unit. These outliers generally consist of Upper Triassic platform carbonates. One of them, the Csóvár block, also contains slope and basinal facies of the Upper Triassic to Lower Jurassic

Csóvár Limestone Formation (Fig. 1). Rhaetian rocks are exposed in the Pokolvölgy quarry (Haas et al., 1997). Partly correlative and younger strata, ranging in age to Early Jurassic (Kozur, 1993), crop out on the southwestern slope of Várhegy, where a Tr-J boundary section was located and exposed by a trench (Pálffy and Dosztály, 2000).

On the basis of field observations and microfacies analysis, 11 lithofacies types have been distinguished in the section (Fig. 2), permitting reconstruction of the sedimentary history. In the lowermost part (0–12 m), proximal and distal turbidite layers alternate with radiolarian basin facies, indicating a distal toe-of-slope depositional environment. It is followed by laminites of very distal turbidite origin, containing a few small slump balls (12–18.7 m), and an interval of filament-rich basinal facies (18.7–20.1 m). The next interval (20.1–22.4 m) begins with a thin debris-flow layer that is overlain by distal turbidites. Radiolarian basinal deposits show slump structures from 22.4 to 25.4 m. A filament-rich basinal facies prevails between 25.4 and 31.8 m.

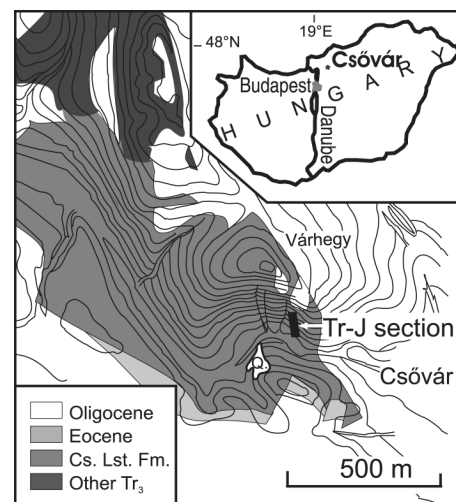


Figure 1. Location of Triassic-Jurassic (Tr-J) boundary section at Csóvár. Geology of southeast part of Csóvár block is simplified from Benkő and Fodor (2001). Q. is Pokolvölgy quarry; Cs. Lst. Fm. is Csóvár Limestone Formation.

*E-mail: palfy@paleo.nhmus.hu; current address: Hungarian Natural History Museum, POB 137, H-1431 Budapest, Hungary.

It is overlain by a distinctive toe-of-slope facies consisting of mainly redeposited grapestone with mollusk-brachiopod coquina lenses (31.8–33.9 m).

BIOSTRATIGRAPHY

Scarce findings of ammonoids (<30 specimens) permit zonal resolution (Fig. 2). The lowest 10 m of the section is dominated by *Choristoceras* spp. and is assigned to the topmost Triassic Marshi zone (Krystyn, 1987). A float specimen of *Nevadaphyllites* cf. *psilomorphum*,

a species known only from the earliest Jurassic (Guex, 1995), was found at 18.8 m. The stratigraphically lowest ammonoid found in situ indicates that the Hettangian is a psiloceratid that occurs 30 m above the base. *Wahneroceras* sp. at the top of the exposed section, ~20 m above the highest layer sampled for the isotopic study, suggests the presence of the middle Hettangian (Pálffy and Dosztály, 2000).

We collected 20 samples from the lower 32 m of the section and processed them for acid-

insoluble microfossils. Of these, all except one produced microfauna, chiefly conodonts, holothurians, and ichthyoliths. A single bed 1.5 m above the base yielded radiolarians, including *Globolaxtorum tozeri*, index species of the topmost Rhaetian radiolarian zone in North America (E.S. Carter, 2000, personal commun.). Most of the conodonts come from the basal 10 m of the section. This typical Tethyan conodont fauna is dominated by species of *Misikella*. There is a staggered disappearance of the older *M. hernsteini*, the younger *M. posthernsteini*, and *M. ultima*. Most samples contain both of the younger species, which are the nominal species of two zones recognized by Kozur and Mock (1991). The presence of a discrete *M. ultima* zone is suggested only by a single specimen recovered at 21 m. A terminal Triassic conodont zone based on *Neohindeodella detrei* (Kozur and Mock, 1991) could not be confirmed.

The Tr-J boundary is in the 21.1–30.1 m interval, i.e., above the last conodont and below the first Jurassic ammonoid found in place.

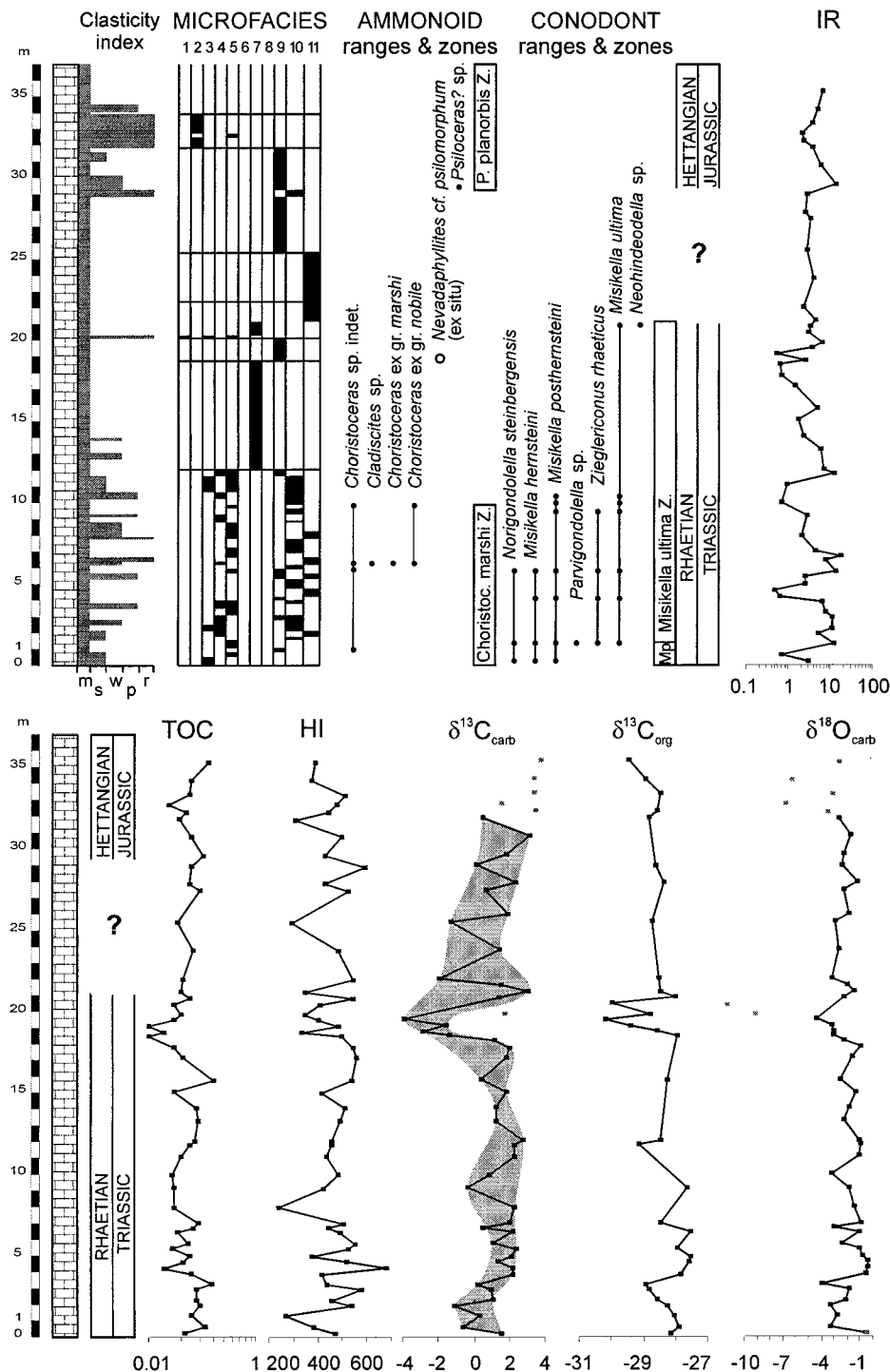


Figure 2. Sedimentology, biostratigraphy, and geochemistry of Triassic-Jurassic boundary section at Csővár. Key to clasticity index: m—0–1 mm mudstone; s—1–2 mm calcareous siltstone; w—2–3 mm calcarenite wackestone; p—3–4 mm calcarenite packstone and grainstone; r—4–5 mm calcirudite. Key to microfacies types and their depositional environment (in parentheses): 1—lithoclastic-bioclastic rudite; 2—redeposited oncoid-grapestone; 3—redeposited bioclastic wackestone (1–3: toe of slope); 4—redeposited bioclastic packstone (proximal turbidite); 5—peloidal packstone (distal turbidite); 6—bioclastic calcareous siltstone (periplatform basin); 7—laminated peloidal wackestone (very distal turbidite); 8—sponge spicule wackestone; 9—filament wackestone; 10—radiolarian wackestone; 11—radiolarian packstone (8–11: basin). Horizontal lines demarcate intervals of basin evolution discussed in text. Abbreviations in biostratigraphy: Z.—zone; Mp—*Misikella posthernsteini* zone. IR—insoluble residue (weight percent); TOC—total organic content (weight percent); HI—hydrogen index. Amount, type, and maturity of organic matter were determined by standard Rock-Eval method on samples decarbonated by HCl treatment. Carbon and oxygen isotope compositions of carbonates were determined on powdered samples by using conventional H_3PO_4 digestion method. Carbon isotope composition of organic matter was determined by mixing decarbonated samples with CuO followed by oxidation at 480 °C for 15 h. $^{13}C/^{12}C$ and $^{18}O/^{16}O$ ratios were determined on evolved CO_2 by using Finnigan MAT delta S mass spectrometer. Results are expressed in delta notation, in per mil (‰) relative to Vienna Pee Dee belemnite standard. Reproducibility is better than $\pm 0.2\text{‰}$. Gray dots mark samples excluded because of diagenetic overprint.

STABLE ISOTOPE AND ORGANIC GEOCHEMISTRY

We collected 53 bulk carbonate samples from 35 m of the biostratigraphically defined uppermost Triassic to lowermost Jurassic strata. The CaCO_3 content exceeds 90% throughout most of the section. The insoluble residue (IR) is composed mostly of silica, presumably derived from radiolarians. Carbon and oxygen isotope compositions of carbonate are listed in Table 1¹ and plotted with other geochemical data along the stratigraphic section in Figure 2. Measured $\delta^{13}\text{C}_{\text{carb}}$ values fluctuate between -3.9‰ and 3.2‰ , although the majority of samples yield values between 0‰ and 2.5‰ . The $\delta^{13}\text{C}_{\text{carb}}$ curve is characterized by oscillations, commonly even between adjacent samples, but this pattern is overridden by a major negative peak in the topmost Triassic and a smaller negative shift at the base of the section, in the Rhaetian. Oxygen isotope ratios are generally between -3.2‰ and -0.2‰ , although some extreme negative values to -10.3‰ were also measured.

Interpretation of the results requires distinction between a primary isotopic signal and a possible diagenetic overprint. Because diagenesis may cause negative $\delta^{18}\text{O}$ shifts that are coupled with ^{13}C depletion (Marshall, 1992), we used a $\delta^{18}\text{O}$ versus $\delta^{13}\text{C}$ plot to detect altered samples (Fig. 3). Although the data distribution indicates that some of the layers may contain exotic material and/or have been diagenetically altered, the negative $\delta^{13}\text{C}_{\text{carb}}$ excursions, the largest of which nearly coincides with the Tr-J boundary, do not appear to be diagenetic in origin and are the main features for further discussion. It is significant that the largest anomaly is not associated with lithologic change.

The total organic carbon content (TOC) is low in the entire section, mostly $<0.1\%$. Rock-Eval maximum temperature values that range between 430 and 442 °C indicate the high end of the immature zone and/or transition to the oil window, suggesting that the kerogen did not undergo strong thermal maturation. The hydrogen index (HI), exceeding 400 mg hydrocarbon per gram of organic carbon throughout most of the section, reveals well-preserved, type II kerogen of predominantly marine origin. The amount of IR covaries with the TOC. In the topmost Triassic, both the TOC and IR show a marked drop, accompanied by a significant decrease in HI. This pattern may suggest a parallel decrease in fluxes of both the marine organic matter (OM) and the radiolarian opal while the relatively minor

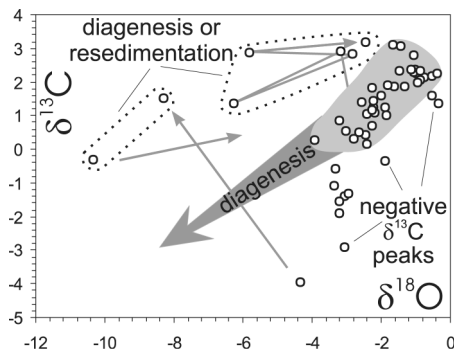


Figure 3. Cross-plot of $\delta^{13}\text{C}$ vs. $\delta^{18}\text{O}$ for bulk carbonate samples from Csóvár section. Arrows mark sudden shifts in adjacent samples toward more negative $\delta^{18}\text{O}$ values. These likely reflect local effects of migrating diagenetic fluids or resedimentation of carbonate and/or influx of meteoric water. Layers with distinctive $\delta^{13}\text{C}$ vs. $\delta^{18}\text{O}$ distribution are platform-derived or slump deposits. These samples (marked by gray dots in Fig. 2) are excluded from further discussion. Majority of samples are clustered along diffuse trend (shaded) corresponding to only initial segment of progressive diagenesis (thick gray arrow) established by Marshall (1992) and Morante and Hallam (1996). Vertical trends involve shifts toward low $\delta^{13}\text{C}$ values that are not associated with significant change in $\delta^{18}\text{O}$ and assumed to be primary.

flux of the hydrogen-poor terrestrial OM remained unchanged.

The $\delta^{13}\text{C}_{\text{org}}$ values range between -30.2‰ and -27.5‰ and show fluctuations similar to those observed in the carbonate data. Here, too, the main feature is a negative peak immediately below the top of Triassic. The negative shift of -2‰ is slightly delayed and of lesser magnitude compared to the $\delta^{13}\text{C}_{\text{carb}}$ anomaly. Another, smaller negative peak near the bottom of the section was investigated at high resolution. It proved that the shift represents a continuous fluctuation in $\delta^{13}\text{C}_{\text{org}}$ that reflects primary variation rather than a random noise in the isotope data. The HI and TOC exhibit no correlation with the $\delta^{13}\text{C}_{\text{org}}$ fluctuation.

DISCUSSION AND CONCLUSIONS

The observed large negative $\delta^{13}\text{C}$ anomaly in both carbonate and organic matter near the Tr-J boundary is significant for models of the end-Triassic extinction and for comparison with similar isotopic events at other extinction boundaries. Possible diagenetic alteration needs to be fully evaluated to ensure that the interpretations are based on the primary isotopic signal. After elimination of the largest negative $\delta^{18}\text{O}$ shifts by excluding samples with suspected diagenetic overprint, the negative $\delta^{13}\text{C}_{\text{carb}}$ excursion and the $\delta^{18}\text{O}$ and $\delta^{13}\text{C}_{\text{carb}}$ fluctuations remain. As diagenesis is expected to shift $\delta^{13}\text{C}_{\text{carb}}$ toward lighter values (Marshall, 1992), a useful conservative

approach is to consider the upper bound of the envelope on the $\delta^{13}\text{C}_{\text{carb}}$ curve (Grötsch et al., 1998). If this method is followed, the main negative excursion of -3.5‰ remains a robust feature (Fig. 2). Because the isotope composition of organic carbon is less prone to diagenetic alteration than that of carbonate carbon, the close parallelism of $\delta^{13}\text{C}_{\text{carb}}$ and $\delta^{13}\text{C}_{\text{org}}$ further supports that both curves represent primary isotopic signals. The rather uniform hydrogen indices throughout the section also indicate that diagenesis has not affected the $\delta^{13}\text{C}_{\text{org}}$ significantly.

Parallel negative $\delta^{13}\text{C}$ excursions in carbonate and organic matter register a shift in the common carbon reservoir, caused by an influx of external CO_2 enriched in ^{12}C . The observed excursion is larger in carbonate (-3.5‰) than in the organic matter (-2‰). Several processes may produce changes in $\Delta^{13}\text{C}$ (i.e., the difference between $\delta^{13}\text{C}_{\text{carb}}$ and $\delta^{13}\text{C}_{\text{org}}$). (1) Elevated temperature results in lower $\delta^{13}\text{C}_{\text{carb}}$ values by reducing the $\text{CO}_{2(\text{g})}$ - HCO_3^- fractionation, but leaves $\delta^{13}\text{C}_{\text{org}}$ unchanged. If the observed $\delta^{18}\text{O}$ variations partly represent changes in seawater temperature, then the main carbon excursion corresponds to a period of warming. McElwain et al. (1999) found paleobotanical evidence for a "super greenhouse" episode at the Tr-J boundary. However, this effect would only account for a fraction of the observed $\delta^{13}\text{C}_{\text{carb}}$ excursion, requiring additional driving forces. (2) Slightly lowered HI values in the boundary layers indicate a relative increase in the amount of terrestrial organic matter, the carbon isotope composition of which is heavier than that of marine kerogen in this period (Lewan, 1986; McElwain et al., 1999), counteracting the process responsible for the negative $\delta^{13}\text{C}$ shift. Consequently, the decrease of the carbon isotope ratio of the marine OM was even more pronounced than suggested by the measured drop of $\delta^{13}\text{C}_{\text{org}}$.

The slight delay of $\delta^{13}\text{C}_{\text{org}}$ excursions compared to the $\delta^{13}\text{C}_{\text{carb}}$ peaks indicates that the dissolved carbonate reservoir was more sensitive to, or the organic carbon reservoir was buffered against, the process that brought about the isotope shifts. Modeling results predict such a time lag even in response to the same forcing (Kump and Arthur, 1999).

In summary, a negative shift of $\sim 3\text{‰}$ is implied in the total exchangeable carbon reservoir near the Tr-J boundary. Previously proposed models attempting to explain such ^{12}C enrichment at other crises invoke decreased bioproductivity and ensuing ^{12}C accumulation in the exchangeable carbon reservoir (Kump and Arthur, 1999), release and oxidation of CH_4 from methane hydrates (Dickens et al., 1995), introduction of large quantities of CO_2 into the atmosphere through intense volcanism

¹GSA Data Repository item 2001121, Geochemical data, is available from Documents Secretary, GSA, P.O. Box 9140, Boulder, CO 80301-9140, editing@geosociety.org, or at www.geosociety.org/pubs/ft2001.htm.

(Kump and Arthur, 1999), sudden turnover of bottom water enriched in dissolved CO₂ derived from decomposition of organic matter (Knoll et al., 1996), or voluminous release of CO₂ through oxidation of organic matter (Magaritz et al., 1992).

Applicability of the last hypothesis is contradicted by the lack of change in the quality of OM. The oceanic-turnover model predicts widespread anoxic sediments; this is not borne out by the stratigraphic record at the Tr-J boundary. Although intense volcanism of the Central Atlantic magmatic province is thought to be connected with the end-Triassic extinction (Marzoli et al., 1999; Pálffy et al., 2000), it would affect the atmospheric pCO₂ but cannot account for the observed change in the isotopic composition (Kump and Arthur, 1999). A productivity crisis and a sudden release of methane through dissociation of gas hydrates are both possible, and not mutually exclusive, explanations of the observed isotopic and fossil record.

Negative carbon isotope anomalies are well known from the Cretaceous-Tertiary boundary, where they have been traditionally ascribed to reduction in the primary productivity (Kump, 1991). However, the most distinctive isotopic feature of the end-Cretaceous extinction, the disappearance of a surface to deep-water carbon isotope gradient, is difficult to recognize in pre-Cretaceous extinctions, where deep-sea sediments are not readily available. Radiolarian faunal change recorded at the Tr-J boundary (Pálffy et al., 2000) and selectivity in bivalve extinction (McRoberts and Newton, 1995) suggest that the base of the marine food web was severely affected. Changes of TOC, IR, and $\Delta^{13}\text{C}$ in the studied section are also tentatively interpreted to reflect reduced productivity.

Several recent studies have suggested that sharp, sudden, negative $\delta^{13}\text{C}_{\text{carb}}$ and $\delta^{13}\text{C}_{\text{org}}$ shifts may be best explained by methane release from gas hydrates. The magnitude and short duration of the main negative anomaly reported here are comparable to the isotope excursions of other intervals for which methane release was hypothesized, e.g., the late Paleocene (Dickens et al., 1995), Toarcian (Hesselbo et al., 2000), and end-Permian (Krull and Retallack, 2000). In all cases, negative carbon anomalies are coeval with large igneous province formation, although the magnitude of concomitant extinction is different. A possible negative terrestrial $\delta^{13}\text{C}_{\text{org}}$ anomaly at the Tr-J boundary (McElwain et al., 1999) may support application of this model, for which no direct tests have been developed yet. Volcanism of the Central Atlantic magmatic province may have induced climatic and oceanographic changes that triggered gas hydrate dissociation, which in turn accelerated

environmental change, contributing to the biotic turnover around the Tr-J boundary.

A Tr-J boundary event is recognizable in the isotope record. Although the ultimate cause remains unsolved, both the productivity collapse and the methane-release models predict a global isotopic signal. Indeed, our data from a Tethyan section are similar to those from a Pacific locality (Ward et al., 2001). Studies from other geographic areas and different environmental settings will help us better understand the end-Triassic perturbation of the global carbon cycle.

ACKNOWLEDGMENTS

The late L. Dosztály helped with field work; E.S. Carter identified the radiolarian faunas. We thank M. Aberhan, S. Hesselbo, and A. von Hillebrandt for fruitful discussions, and C. McRoberts for a helpful review. Financial support was provided by the Hungarian Scientific Research Fund (grants F023451, T029797, and T034168) and the Humboldt Foundation. This is a contribution to International Geological Correlation Programme Project 458.

REFERENCES CITED

- Benkő, K., and Fodor, L., 2001, Late Cretaceous–middle Eocene compressional deformation in the NE part of the Transdanubian Unit, Hungary: *Hungarian Geological Society Bulletin*, v. 131 (in press).
- Dickens, R.G., O'Neil, J.R., Rea, D.K., and Owen, R.M., 1995, Dissociation of oceanic methane hydrate as a cause of the carbon isotope excursion at the end of the Paleocene: *Paleoceanography*, v. 10, p. 965–971.
- Grötsch, J., Billing, I., and Vahrenkamp, V., 1998, Carbon-isotope stratigraphy in shallow-water carbonates: Implications for Cretaceous black-shale deposition: *Sedimentology*, v. 45, p. 623–634.
- Guxé, J., 1995, Ammonites hettangiennes de la Gabbs Valley Range (Nevada, USA): *Mémoires de Géologie (Lausanne)*, v. 27, 131 p.
- Haas, J., Tardi-Filác, E., Oravecz-Scheffer, A., Góczán, F., and Dosztály, L., 1997, Stratigraphy and sedimentology of an Upper Triassic toe-of-slope and basin succession at Csővár, North Hungary: *Acta Geologica Hungarica*, v. 40, p. 111–177.
- Hallam, A., 1996, Major bio-events in the Triassic and Jurassic, in Walliser, O.H., ed., *Global events and event stratigraphy in the Phanerozoic*: Berlin, Springer, p. 265–283.
- Hallam, A., and Goodfellow, W.D., 1990, Facies and geochemical evidence bearing on the end-Triassic disappearance of the Alpine reef ecosystem: *Historical Biology*, v. 4, p. 131–138.
- Hallam, A., and Wignall, P.B., 1997, Mass extinctions and their aftermath: Oxford, Oxford University Press, 320 p.
- Hesselbo, S.P., Gröcke, D.R., Jenkyns, H.C., Bjerum, C.J., Farrimond, P., Morgans Bell, H.S., and Green, O.R., 2000, Massive dissociation of gas hydrate during a Jurassic oceanic anoxic event: *Nature*, v. 406, p. 392–395.
- Knoll, A.H., Bambach, R.K., Canfield, D.E., and Grotzinger, J.P., 1996, Comparative Earth history and Late Permian mass extinction: *Science*, v. 273, p. 452–457.
- Kozur, H., 1993, First evidence of Liassic in the vicinity of Csővár (Hungary), and its paleogeographic and paleotectonic significance: *Jahrbuch der Geologischen Bundesanstalt*, v. 136, p. 89–98.

- Kozur, H., and Mock, R., 1991, New Middle Carnian and Rhaetic conodonts from Hungary and the Alps: Stratigraphic importance and tectonic implications for the Buda Mountains and adjacent areas: *Jahrbuch der Geologischen Bundesanstalt*, v. 134, p. 271–297.
- Krull, E.S., and Retallack, G.J., 2000, $\delta^{13}\text{C}$ depth profiles from paleosols across the Permian-Triassic boundary: Evidence for methane release: *Geological Society of America Bulletin*, v. 112, p. 1459–1472.
- Krystyn, L., 1987, Zur Rhät-Stratigraphie in den Zlam-bach-Schichten (vorläufiger Bericht): *Sitzungsberichte der Österreichischen Akademie der Wissenschaften, Mathematisch-naturwissenschaftliche Klasse, Abteilung I*, v. 196, p. 21–36.
- Kump, L.R., 1991, Interpreting carbon-isotope excursions: Strangelove oceans: *Geology*, v. 19, p. 299–302.
- Kump, L.R., and Arthur, M.A., 1999, Interpreting carbon-isotope excursions: Carbonates and organic matter: *Chemical Geology*, v. 161, p. 181–198.
- Lewan, M.D., 1986, Stable carbon isotopes of amorphous kerogens from Phanerozoic sedimentary rocks: *Geochimica et Cosmochimica Acta*, v. 50, p. 1583–1591.
- Magaritz, M., Krishnamurthy, R.V., and Holser, W.T., 1992, Parallel trends in organic and inorganic carbon isotopes across the Permian/Triassic boundary: *American Journal of Science*, v. 292, p. 727–739.
- Marshall, J.D., 1992, Climatic and oceanographic isotopic signals from the carbonate rock record and their preservation: *Geological Magazine*, v. 129, p. 143–160.
- Marzoli, A., Renne, P.R., Piccirillo, E.M., Ernesto, M., Bellieni, G., and De Min, A., 1999, Extensive 200-million-year-old continental flood basalts of the Central Atlantic magmatic province: *Science*, v. 284, p. 616–618.
- McElwain, J.C., Beerling, D.J., and Woodward, F.I., 1999, Fossil plants and global warming at the Triassic-Jurassic boundary: *Science*, v. 285, p. 1386–1390.
- McRoberts, C.A., and Newton, C.R., 1995, Selective extinction among end-Triassic European bivalves: *Geology*, v. 23, p. 102–104.
- McRoberts, C.A., Furrer, H., and Jones, D.S., 1997, Palaeoenvironmental interpretation of a Triassic-Jurassic boundary section from western Austria based on palaeoecological and geochemical data: *Palaeogeography, Palaeoclimatology, Palaeoecology*, v. 136, p. 79–95.
- Morante, R., and Hallam, A., 1996, Organic carbon isotopic record across the Triassic-Jurassic boundary in Austria and its bearing on the cause of the mass extinction: *Geology*, v. 24, p. 391–394.
- Pálffy, J., and Dosztály, L., 2000, A new marine Triassic-Jurassic boundary section in Hungary: Preliminary results, in Hall, R.L., and Smith, P.L., eds., *Advances in Jurassic research 2000*: Zürich, TransTech, p. 173–179.
- Pálffy, J., Mortensen, J.K., Carter, E.S., Smith, P.L., Friedman, R.M., and Tipper, H.W., 2000, Timing the end-Triassic mass extinction: First on land, then in the sea?: *Geology*, v. 28, p. 39–42.
- Ward, P.D., Haggart, J.W., Carter, E.S., Wilbur, D., Tipper, H.W., and Evans, T., 2001, Sudden productivity collapse associated with the Triassic-Jurassic boundary mass extinction: *Science*, v. 292, p. 1148–1151.

Manuscript received March 15, 2001

Revised manuscript received June 25, 2001

Manuscript accepted July 20, 2001

Printed in USA